Current Research in Food Science 10 (2025) 100992

Contents lists available at ScienceDirect

Current Research in Food Science

journal homepage: www.sciencedirect.com/journal/current-research-in-food-science

Oleraceins from *Portulaca oleracea* leaves: Quali-quantitative determination and antioxidant potential

Ciro Cannavacciuolo [a,b], Assunta Napolitano [a], Verena M. Dirsch [c], Elke H. Heiss [c], Milena Masullo [a], Sonia Piacente [a,d,*]

[a] *Dipartimento di Farmacia, Università Degli Studi di Salerno, Via Giovanni Paolo II n. 132, 84084, Fisciano, SA, Italy*
[b] *PhD Program in Drug Discovery and Development, Università Degli Studi di Salerno, Via Giovanni Paolo II n. 132, I-84084, Fisciano, SA, Italy*
[c] *Department of Pharmaceutical Sciences, University of Vienna, Josef-Holaubek-Platz 2, 1090, Vienna, Austria*
[d] *National Biodiversity Future Center (NBFC), 90133, Palermo, Italy*

ARTICLE INFO

Handling Editor: Professor Aiqian Ye

Keywords:
Portulaca oleracea L.
Purslane
'Green' extracts
Oleraceins
Cyclo-DOPA phenolic alkaloids
Antioxidant activity
Nrf2-activation

ABSTRACT

Portulaca oleracea L. (purslane) is a spontaneous herb whose shoots are appreciated in the Mediterranean and Asian diets for their fresh flavor and crunchy texture. In addition to PUFA (PolyUnsaturated Fatty Acids), it contains unusual polyphenolic alkaloids called oleraceins. This work aimed at investigating the oleracein profile of different 'green' extracts of the leaves of *Portulaca oleracea* and evaluating their antioxidant capacity. An LC-MS screening of different extracts revealed the infusion as the extract richest in oleraceins. Qualitative and quantitative analysis of oleraceins in this extract resulted in the identification of three polyphenolic alkaloids never reported before and in the definition of oleracein A as the most abundant alkaloid. An oleracein-enriched fraction from the infusion and its hydrolysed derivative exhibited radical scavenging activity *in vitro* and led to activation of the Nrf2 pathway in cells without apparent cytotoxicity. Thus, its oleracein content may make purslane a potential nutraceutical for alleviating redox distress.

1. Introduction

Portulaca oleracea L. (purslane), a spontaneous herb with edible reddish stems and alternate leaves, is widespread in temperate and tropical areas of the world (Melilli et al., 2020), and is particularly appreciated as a salad in the Mediterranean and Asian diets for the fresh taste and crisp texture of its shoots (Cannavacciuolo et al., 2022).

Due to its ready availability, this plant has also been used as a folk medicine in different parts of the world to alleviate a wide range of ailments, including diabetes, gastrointestinal, cardiovascular diseases, and hepatitis (Kumar et al., 2022; Iranshahy et al., 2017; Yang et al., 2024; Ma et al., 2024). Its medicinal properties have been known since ancient times, e.g., they have been reported in the manuscript "le Pandette", a collection of medicinal plants used as the basis of the ancient "Schola Medica Salernitana", mentioned in numerous landmark medical textbooks, and listed in various pharmacopeias (Kumar et al., 2022; Iranshahy et al., 2017). Consistent with its ethnomedicinal properties, several scientific studies based on *in vitro* and *in vivo* tests have confirmed the efficacy of purslane as a medicinal plant and have provided interesting results on its bioactivity (Kumar et al., 2022; Rahimi et al., 2019). Our previous study highlighted *P. oleracea* as a source of polar lipids ranging from linear and cyclic oxylipins to high molecular weight lipids including glycolipids, phospholipids and sphingolipids. The evaluation of their anti-inflammatory potential by *in vitro* reporter gene assays showed that purslane lipid-enriched fractions, at a concentration of 20 μg/ml, inhibit the TNF-α-stimulated NF-kB pathway and induce the activation of PPAR-ɣ and Nrf2 transcription factors (Cannavacciuolo et al., 2022).

Particular attention has been paid to the neuroprotective capacity of *P. oleracea*. Several preclinical studies have shown that polar extracts of purslane exert neuroprotective activity, probably due to their antioxidant capacity, in some cases attributing the bioactivity to betacyanins, i.e. red-violet water-soluble nitrogen-containing pigments belonging to the betalain class (Iranshahy et al., 2017; Truong et al., 2019; Moneim, 2013; Moneim et al., 2013; Zhang et al., 2007; Wang and Yang, 2010; Wang et al., 2007; Farag and Shakour, 2019). Using *in vitro* and *in vivo* models, Sun et al. described the neuroprotective potential of oleracein E which protected dopaminergic neurons against rotenone toxicity by

* Corresponding author. Dipartimento di Farmacia, Università degli Studi di Salerno, Via Giovanni Paolo II n. 132, 84084, Fisciano, SA, Italy.
E-mail address: piacente@unisa.it (S. Piacente).

https://doi.org/10.1016/j.crfs.2025.100992
Received 7 November 2024; Received in revised form 24 January 2025; Accepted 29 January 2025
Available online 30 January 2025
2665-9271/© 2025 Published by Elsevier B.V. This is an open access article under the CC BY-NC-ND license (http://creativecommons.org/licenses/by-nc-nd/4.0/).

reducing oxidative stress (Sun et al., 2017). Oleracein E is a representative of the oleraceins, which may have higher or similar antioxidant capacity than some natural antioxidants such as vitamin C and vitamin E (Kumar et al., 2022; Fernández-Poyatos et al., 2021; Jiao et al., 2015). Structurally, oleraceins are cyclo-DOPA phenolic alkaloids mainly characterised by a 5,6-dihydroxyindoline-2-carboxylic acid nucleus *N*-acylated with cinnamic acid derivatives and glycosylated with one or more glucose units, showing the same scaffold as the yellow water-soluble pigments betaxanthins, the other member of the betalains class (Farag and Shakour, 2019; Fernández-Poyatos et al., 2021; Jiao et al., 2014; Tanaka et al., 2008).

Therefore, based on these considerations and on the widespread use of purslane leaves in various culinary recipes of the Mediterranean area, different green extracts of the leaves of *P. oleracea,* endemic to southern Italy, were analysed with the aim to define the most selective extraction procedure towards oleraceins and to evaluate the quality and quantity of these unusual polyphenolic alkaloids. Furthermore, their antioxidant capacity, i.e. their potential to scavenge radicals and to support the cellular antioxidant stress response, was evaluated. For the latter, we focused on the activation of the transcription factor Nrf2 (nuclear factor E2 -related factor 2), which is a key regulator of genes involved in detoxification, repair and elimination of oxidative damage and is emerging as a viable target in the prevention of chronic degenerative diseases (Cuadrado et al., 2019).

2. Materials and methods

2.1. Chemicals and instrumental equipments

For chemicals and instrumental equipment used for NMR experiments and data processing, HPLC-UV separations, and antioxidant assays, see section S1 of the Supplementary materials.

2.2. Plant sample

Approximately 1 kg of *P. oleracea* aerial parts were randomly harvested in June 2019 (month average temperature and humidity: 22.8 °C and 77.1 %, respectively) from a natural spontaneous population in Gragnano (Naples, Italy; GPS coordinates 40°42′15″N 14°30′55″E, 74 a.s.l.). Prof. V. De Feo, botanist of the Department of Pharmacy, University of Salerno, identified the plant; a voucher specimen is preserved at the same institution.

2.3. Sample preparation procedures

The leaves of at least 20 plants per replicate (3) of *P. oleracea* were separated by hand from the stems, cleaned, and dried in a forced-air oven at 40 °C to constant weight. Different 'green' extracts were then prepared from 5.0 g of dried leaves each. Specifically, ethanol, ethanol-water mixtures (70% and 50%, v/v), and water were used to extract the leaves by maceration at room temperature (50 mL x 3 days × 3 times). At the same time, infusion and decoction were prepared according to the procedures of the Official European Pharmacopoeia. The extracts were then filtrated and dried under vacuum by Rotavapor. 1.25 g, 1.10 g, and 0.90 g of extracts were obtained from infusion, water maceration, and decoction, respectively, while ethanol, 70% ethanol, and 50% ethanol extracts yielded 0.90 g, 1.10 g, and 1.15 g of extracts, respectively.

To obtain an oleracein-enriched fraction, 1 g of infusion was dissolved in 1 mL of MeOH/H_2O (20:80, v/v), centrifuged and the supernatant was fractionated on a Sep-Pak C-18 cartridge (Strata C18, 10 g, 55 μm, 70 Å, from Phenomenex) by using CH_3CN/H_2O (v/v) in different ratios (10%, 30%, 50% and 100% ACN, respectively) as solvent. Four fractions of 723 mg, 100 mg, 17 mg, and 3 mg, respectively, were obtained by solid phase extraction (SPE). To enable the cleavage of sugar moieties, 20 mg of the fraction obtained by using 30% ACN was subjected to acid hydrolysis using 5 ml of the Kiliani reagent (HCl:HCOOH: H_2O = 10:35:55 *v/v*), at 100 °C (Mair et al., 2018). After 2h, the solution was cooled down, partitioned between ethyl acetate/water, and the ethyl acetate fraction was dried under vacuum, yielding 14.2 mg.

2.4. ESI/HRMS^n and LC-ESI/HRMS^n qualitative analysis

Liquid chromatography coupled to electrospray ionisation and high resolution multi-stage mass spectrometry (LC-ESI/HRMS^n) analyses were performed in negative ion mode using the instrument, parameters, and conditions reported in the Supplementary materials S2 (Cannavacciuolo et al., 2022).

2.5. Determination of antioxidant activity by TEAC and DPPH assays

The antioxidant activity was determined by the spectrophotometric Trolox Equivalent Antioxidant Capacity (TEAC) assay as previously reported (D'Urso et al., 2020) (see section S3 in the Supplementary materials). The free radical scavenging activities of the tested samples and ascorbic acid (positive control) were measured using the stable 1, 1-diphenyl-2-picrylhydrazyl radical (DPPH$^•$) as previously described (D'Urso et al., 2020; Cerulli et al., 2021) (see section S3 in the Supplementary materials).

2.6. Assessment of Nrf2 activation in a reporter gene assay

Activation of the Nrf2 pathway by extracts/fractions of interest was assessed by a ARE-LUC- reporter gene assay as detailed by Cannavacciuolo et al. (2022) and briefly described in section S4 of the Supplementary materials.

2.7. Isolation of oleraceins

The HPLC-UV separation of the oleracein-enriched fraction (80 mg) was performed by the method reported in section S5 of the Supplementary materials, including column, mobile phases, and gradient conditions, and yields of isolated compounds.

2.8. LC-ESI/QTrap/MS/MS quantitative analysis

The analyses were performed using the instrument and ion spray experimental conditions described by Cerulli et al., 2023. The analytical parameters were optimised using the direct injection mode as described in section S6 of the Supplementary materials. Detailed information on the LC-MS/MS conditions, including the chromatographic method and the Multiple Reaction Monitoring (MRM) experiment settings, is provided in the same section. Calibration curves of standard solutions prepared from the isolated oleraceins were constructed as described in section S7 of the Supplementary materials ($R^2 \geq 0.997$), which also supports information on the determination of limits of detection (LODs) and quantification (LOQs). The results are shown in Table 3.

2.9. Statistical analysis

Each LC-HRMS and LC-MRM-MS experiment was performed in triplicate. Analysis of variance (ANOVA) and *t*-test were used to estimate differences (considered to be significant at $p \leq 0.05$). Microsoft Excel 2016 was used for statistical analyses. For biological assays, three independent *in vitro* assays were performed, each in four technical replicates. The transactivation activity was expressed as mean ± SD of three independent experiments, n = 3, ****$p < 0.0001$ (One-way ANOVA with Dunnett's post hoc test *vs* vehicle control). Statistics were evaluated using GraphPad Prism 9.2.0.

3. Results and discussion

3.1. 'Green extracts' and oleracein-enriched fraction: preparation and qualitative mass spectrometric analyses

To investigate different solvents for selective extraction of the polyphenolic alkaloid class, 'green' solvents such as ethanol, ethanol/water (70% and 30%, *v/v*) mixtures, and water were used. The extracts were obtained by maceration, infusion, and decoction and analysed by ESI/HRMS^n (Fig. 1). In accordance with literature data, the mass range from 500 to 1000 Da was carefully examined in search of $[M-H]^-$ ions, yielding tandem mass spectra characterised by the appearance of diagnostic oleracein product ions corresponding to the cyclo-DOPA anion or to ions formed by neutral loss of typical oleracein moieties, such as coumaroyl, caffeoyl, and feruloyl moieties, together with hexose units (Fig. 1) (Jiao et al., 2014; Voynikov et al., 2021). This analytical approach allowed us to quickly define the infusion as the 'green' extract, characterised by the best selectivity for polyphenolic alkaloids (marked with a green dot in Fig. 1). The hydro-alcoholic extracts showed poor, and in some cases no selectivity for oleraceins and other metabolite classes, such as complex polar lipids (marked with a yellow dot in Fig. 1) (Cannavacciuolo et al., 2022).

The LC-ESI/HRMS^n analysis of the infusion revealed a metabolite distribution in three well-separated time ranges, which account for the elution of several known *P. oleracea* metabolites (Cannavacciuolo et al., 2022; Fernández-Poyatos et al., 2021; Zhang et al., 2022; Nemzer et al., 2020): 1) organic acids (such as gluconic, glucaric, and citric acids), derivatives of hydroxybenzoic acids (such as e.g. dihydroxybenzoic acid hexoside and dihydroxybenzoic acid pentoside), and coumaroyl conjugates of organic acids (such as e.g. coumaroylglucaric acid), all eluted in the first 9 min of the chromatogram, 2) oleraceins, mainly appearing from 9 to 20 min, and 3) oxylipins and fatty acids, eluted from 20 min onwards (Fig. 2, A panel).

Based on this result, the infusion was subjected to SPE using a C18 cartridge and different mixtures of CH_3CN/H_2O (*v/v*) as solvents to obtain a fraction rich in oleraceins for further in-depth structural analysis, including also minor oleraceins. Compared with the LC-ESI/HRMS profile of the infusion, the fraction eluted with 30% ACN showed an increase in the number of peaks eluted in the oleracein region (i.e. from 9 to 20 min) together with a decrease, and in some cases disappearance, of peaks at low and high retention times (Fig. 2, panel B). This fraction was defined as the richest in oleraceins (hereafter referred to as 'oleracein-enriched fraction'), confirming the preliminary results obtained by its ESI/HRMS^n.

Analysis of the molecular formulae and fragmentation patterns of the detected peaks, in comparison with literature data, allowed us to tentatively identify eleven oleraceins (**1**, **3**–**6**, **9**–**14**) previously reported in *P. oleracea* leaves (Farag and Shakour, 2019; Fernández-Poyatos et al., 2021; Jiao et al., 2015; Voynikov et al., 2021; Xiang et al., 2005), and three oleraceins (**2**, **7**–**8**) that, to our knowledge, have never been

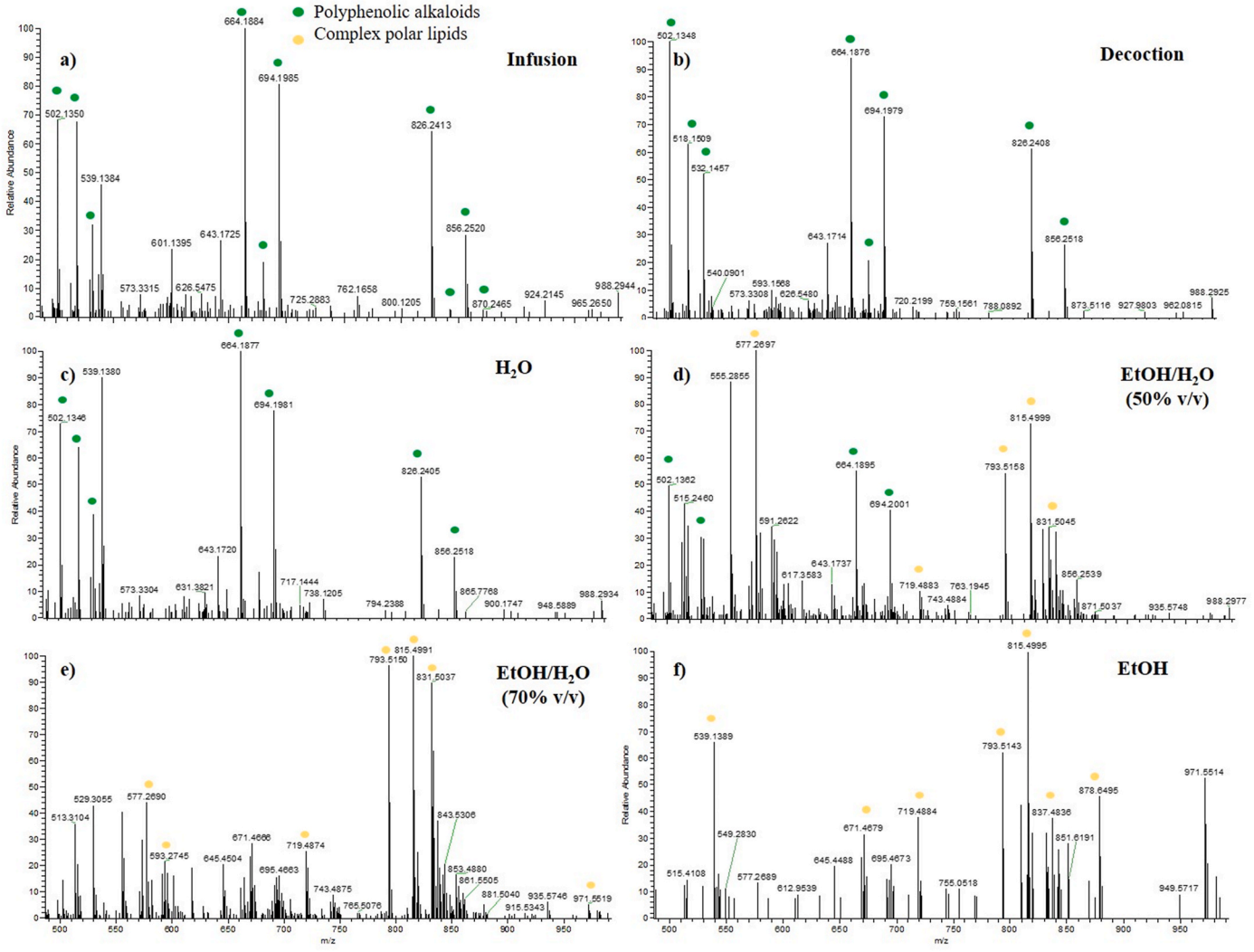

Fig. 1. ESI/HRMS spectra of 'green' extracts of *Portulaca oleracea* leaves obtained *via* a) infusion, b) decoction, and c-f) maceration.

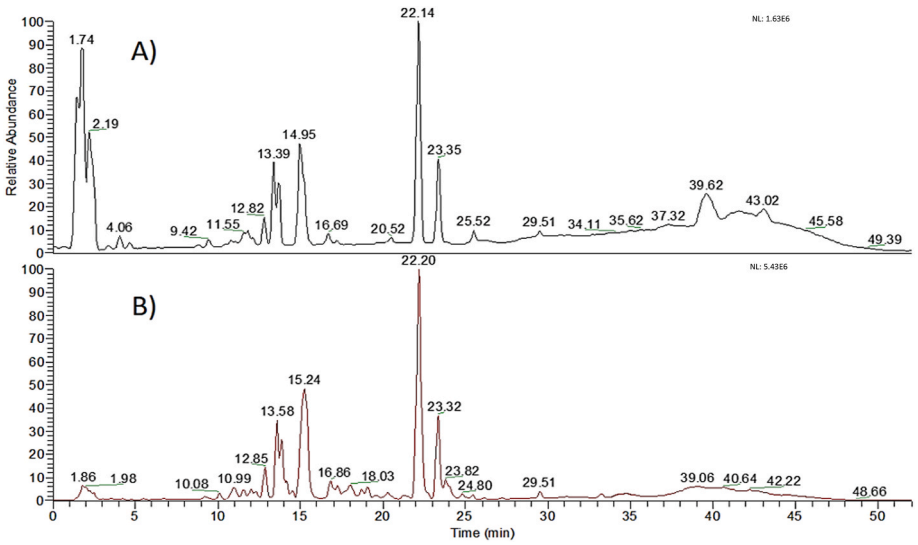

Fig. 2. LC-ESI/HRMS base peak chromatograms of the infusion (A), Normalised Level (NL) 1.63E6, and of the oleraceins-enriched fraction (B), NL 5.43E6, obtained from purslane leaves.

described before (Table 1; Fig. 3). In particular, several metabolites, although having the same *m/z* value and molecular formula, eluted at different times and showed a different fragmentation pattern, allowing us to define them as isomers. This was the case, e.g., for compounds **1** and **7,** which eluted at R_t 10.07 and 12.87 min (Table 1), respectively. Accurate analysis of the tandem mass spectra of compound **1** (*m/z* 826.2399, $C_{36}H_{45}O_{21}N$) revealed a major product ion at *m/z* 664.1874, corresponding to the molecular formula $C_{30}H_{34}O_{16}N$, formed by neutral loss of one hexose unit, together with minor product ions at *m/z* 502.1343 ($C_{24}H_{24}O_{11}N$), formed by neutral loss of two hexose units, at *m/z* 340.0817 ($C_{18}H_{14}O_6N$), formed by neutral loss of three hexose units, and at *m/z* 518.1500 ($C_{21}H_{28}O_{14}N$), formed by neutral loss of one hexose and one coumaroyl unit (Table 1). The detection of the fragment ions at *m/z* 518.1502 ($C_{21}H_{28}O_{14}N$) and *m/z* 340.0817 ($C_{18}H_{14}O_6N$) in the $HRMS^3$ spectrum obtained for the product ion at *m/z* 664.1890, and the absence of the product ion formed by the neutral loss of a single hexose, allowed us to estimate that in **1,** one of the three hexoses had to be located on the *p*-OH of the coumaroyl unit, in turn, *N*-acylated to the cyclo-DOPA scaffold, while the other two had to be linked to each other, being lost as a whole group of 324 Da, and thus located at the 6-OH position of the 5,6-dihydroxyindoline-2-carboxylic acid core. Overall, this fragmentation pattern allowed us to identify **1** as the already known oleracein P (Table 1) (Voynikov et al., 2021). On the contrary, the tandem mass spectrum of compound **7** showed a unique product ion at *m/z* 680.2035, formed by the neutral loss of a coumaroyl moiety and corresponding to the molecular formula $C_{27}H_{38}O_{19}N$ (Table 1), the presence of which allowed us to estimate that the coumaric moiety was not glycosylated. Moreover, the analysis of the $HRMS^3$ spectrum allowed the detection of the product ions at *m/z* 662.1915 ($C_{27}H_{36}O_{18}N$), formed by the neutral loss of a water molecule, at *m/z* 636.2147 ($C_{26}H_{38}O_{17}N$), formed by the neutral loss of a CO_2 molecule, at *m/z* 518.1520 ($C_{21}H_{28}O_{14}N$), formed by neutral loss of a single hexose unit, and at *m/z* 194.0451 ($C_9H_8O_4N$), corresponding to the 5,6-dihydroxyindoline-2-carboxylate anion and produced by neutral loss of three joint hexose units. This mass spectrometric behavior of **7** indicated the presence of three hexose units linked by different interglycosidic bonds, two of which were lost, in agreement with data reported in the literature for other oleraceins, as a whole neutral group of 324 Da being linked *via* a 1‴→6″-interglycosidic linkage, and the other one was lost as a single unit, being involved in a 1⁗→4‴-interglycosidic linkage, as in

Table 1
Oleraceins tentatively identified in the oleraceins-enriched fraction of *Portulaca oleracea* leaves.

n	Compound	R_t (min)	$[M-H]^-$	Molecular formula	Error (ppm)	$HRMS^n$
1	Oleracein P[a]	10.08	826.2399	$C_{36}H_{45}O_{21}N$	−0.20	664.1874 ($C_{30}H_{34}O_{16}N$); 518.1500 ($C_{21}H_{28}O_{14}N$); 502.1343 ($C_{24}H_{24}O_{11}N$); 340.0817 ($C_{18}H_{14}O_6N$). MS^3 (664.1895): 518.1502 ($C_{21}H_{28}O_{14}N$); 340.0817 ($C_{18}H_{14}O_6N$)
2	Oleracein α	10.39	664.1880	$C_{30}H_{35}O_{16}N$	1.26	340.0832 ($C_{18}H_{14}O_6N$)
3	Oleracein Q[a]	11.08	856.2509	$C_{37}H_{47}O_{22}N$	1.65	694.1981 ($C_{31}H_{36}O_{17}N$); 532.1447 ($C_{25}H_{26}O_{12}N$); 518.1506 ($C_{21}H_{28}O_{14}N$); 370.0925 ($C_{19}H_{16}O_7N$)
4	Oleracein I isomer	11.54	694.1981	$C_{31}H_{37}O_{17}N$	0.41	518.1515 ($C_{21}H_{28}O_{14}N$); 370.0939 ($C_{19}H_{16}O_7N$)
5	Oleracein C[a]	11.61	664.1880	$C_{30}H_{35}O_{16}N$	1.17	502.1349 ($C_{24}H_{24}O_{11}N$); 340.0831 ($C_{18}H_{14}O_6N$)
6	Oleracein β	12.32	680.1830	$C_{30}H_{35}O_{17}N$	1.26	518.1296 ($C_{24}H_{24}O_{12}N$); 356.0768 ($C_{18}H_{14}O_7N$). MS^3 (518.1296): 356.0769 ($C_{15}H_{18}O_9N$)
7	Oleracein γ	12.85	826.2410	$C_{36}H_{45}O_{21}N$	1.21	680.2035 ($C_{27}H_{38}O_{19}N$). MS^3 (680.2035): 662.1915 ($C_{27}H_{36}O_{18}N$); 636.2147 ($C_{26}H_{38}O_{17}N$); 518.1520 ($C_{21}H_{28}O_{14}N$); 194.0451 ($C_9H_8O_4N$)
8	Oleracein δ	13.12	856.2513	$C_{37}H_{47}O_{22}N$	0.80	680.2013 ($C_{27}H_{38}O_{19}N$); 370.0915 ($C_{19}H_{16}O_7N$)
9	Oleracein H[a]	13.57	664.1885	$C_{30}H_{35}O_{16}N$	1.08	518.1500 ($C_{21}H_{28}O_{14}N$); 340.0820 ($C_{18}H_{14}O_6N$)
10	Oleracein I[a]	13.87	694.1987	$C_{31}H_{37}O_{17}N$	1.38	518.1503 ($C_{21}H_{28}O_{14}N$); 370.0927 ($C_{19}H_{16}O_7N$)
11	Oleracein A[a]	15.12	502.1349	$C_{24}H_{25}O_{11}N$	0.94	356.0984 ($C_{15}H_{18}O_9N$); 340.0822 ($C_{18}H_{14}O_6N$); 296.0922 ($C_{17}H_{14}O_4N$); 194.0454 ($C_9H_8O_4N$)
12	Oleracein B[a]	15.38	532.1454	$C_{27}H_{27}O_{12}N$	0.94	370.0927 ($C_{19}H_{16}O_7N$); 356.0986 ($C_{15}H_{18}O_9N$); 326.1029 ($C_{18}H_{16}O_5N$)
13	Oleracein N/S	17.49	840.2340	$C_{40}H_{43}O_{19}N$	−0.65	694.1930 ($C_{31}H_{36}O_{17}N$)
14	Oleracein O isomer	17.60	870.2459	$C_{41}H_{45}O_{20}N$	−1.41	694.1999 ($C_{31}H_{36}O_{17}N$)

[a] Oleraceins isolated and characterised by 1D and 2D-NMR experiments.

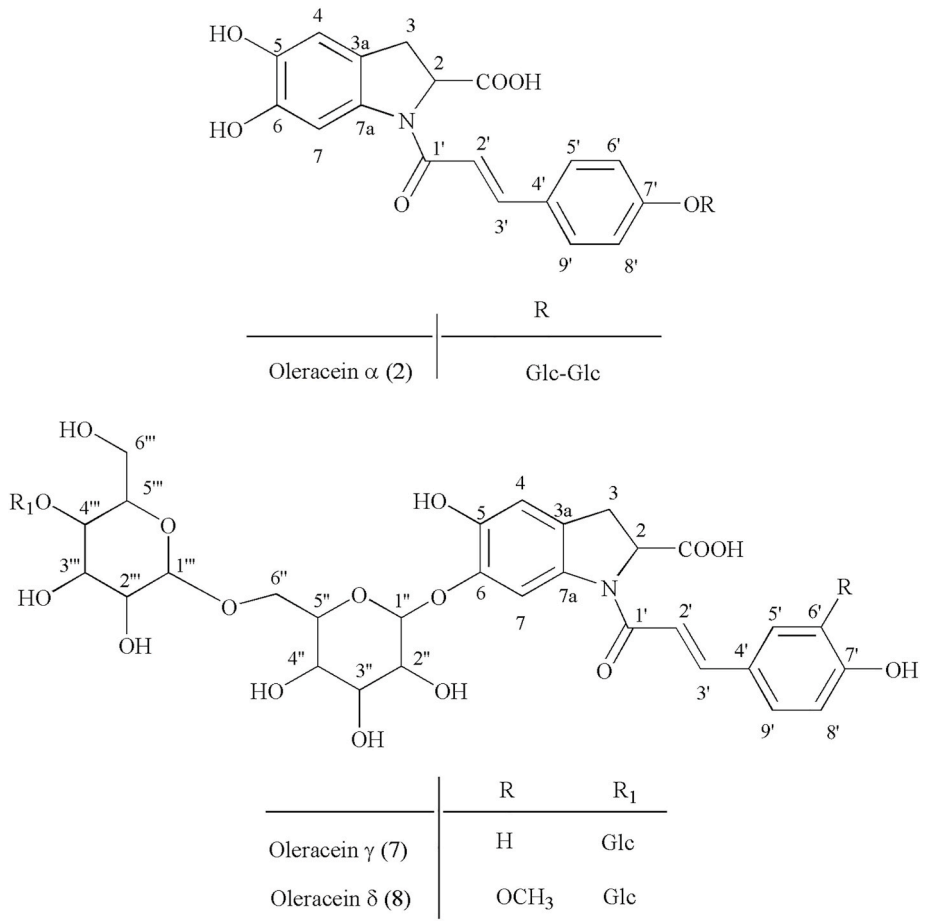

Fig. 3. Proposed structures of *Portulaca* oleraceins α, γ, and δ.

oleraceins Y, Z, ZA and ZB (Voynikov et al., 2021). Therefore, compound **7** was tentatively identified as a new oleracein, named oleracein γ (Table 1; Fig. 3).

Analogously, compounds **3** and **8** showed the same molecular formula but different tandem mass spectra (Table 1). In the HRMS/MS analysis of **3**, the occurrence of the major product ion at *m/z* 694.1981 ($C_{31}H_{36}O_{17}N$), formed by neutral loss of a hexose moiety, together with that of a minor product ion at *m/z* 518.1506 ($C_{21}H_{28}O_{14}N$), formed by neutral loss of a hexose and a feruloyl moiety, suggested that the latter moiety must be glycosylated at the *p*-OH position. Moreover, the detection of a minor product ion at *m/z* 532.1447 ($C_{25}H_{26}O_{12}N$), obtained by neutral loss of two hexose units, together with that at *m/z* 370.0925 ($C_{19}H_{16}O_7N$), obtained by neutral loss of three hexoses, allowed us to identify compound **3** as the known oleracein Q (Table 1) (Voynikov et al., 2021). In contrast, compound **8** yielded a tandem mass spectrum characterised by the main product ion at *m/z* 680.2013 ($C_{27}H_{38}O_{19}N$), generated by neutral loss of a feruloyl moiety, which must therefore be unglycosylated (Table 1). Moreover, the detection of a single minor product ion at *m/z* 370.0915 ($C_{19}H_{16}O_7N$), formed by the neutral loss of three hexose units, and the absence of product ions formed by the neutral loss of one or two hexoses, suggested that, analogously to compound **7**, the three sugars had to be linked together, leading to the conclusion that compound **8** was a new oleracein, named oleracein δ (Table 1; Fig. 3).

Once again, the analysis of the relative $HRMS^n$ spectra allowed us to distinguish three compounds, **2**, **5** and **9**, which have the same molecular formula (Table 1). In the case of **5**, the appearance of a major product ion at *m/z* 502.1349 ($C_{24}H_{24}O_{11}N$), together with a minor one at *m/z* 340.0831($C_{18}H_{14}O_6N$), allowed us to identify **5** as the known oleracein C, structurally characterised by the presence of a 5,6-dihydroxyindoline-2-carboxylic acid *N*-acylated with a mono-glycosylated coumaroyl moiety and a second hexose moiety at the 6-OH position of the indoline amide backbone (Voynikov et al., 2021). On the contrary, the analysis of the HRMS/MS spectrum of compound **9** (Table 1) allowed us to conclude that, in this case, the coumaroyl unit was not glycosylated, with the main product ion at *m/z* 518.1500 ($C_{21}H_{28}O_{14}N$) formed by the cleavage of this cinnamoyl moiety, and that the two hexose units were linked to each other, as evidenced by the product ion formed by their cleavage as a whole group (neutral loss of 324 Da). Overall, this fragmentation pattern allowed us to tentatively assign **9** as the known oleracein H (Voynikov et al., 2021). Compound **2** gave a distinct tandem mass spectrum, characterised by only one main product ion at *m/z* 340.0832 ($C_{18}H_{14}O_6N$), without any product ion formed by neutral loss of single hexose or coumaroyl unit, allowing us to assume that the latter must be glycosylated and that the two hexoses must be linked (Table 1). In this way, compound **2** could be tentatively identified as a new oleracein, named oleracein α (Fig. 3).

It is noteworthy that, unlike the compounds previously studied, both **4** and **10** had the same molecular formula and the same tandem mass spectrum, characterised by a major product ion at *m/z* 518.1503 ($C_{21}H_{28}O_{14}N$), formed by the neutral loss of a ferulic moiety, and by a minor one at *m/z* 370.0927 ($C_{19}H_{16}O_7N$), formed by the neutral loss of two linked hexose units. This fragmentation pattern confirmed the presence of an unglycosylated ferulic unit and of an indoline amide backbone diglycosylated at the 6-OH position (Table 1; Fig. 3), as already observed in oleracein I and its isomer (Voynikov et al., 2021).

3.2. Evaluation of antioxidant activity of purslane infusion and derived fractions

3.2.1. Radical scavenging activity

Both the infusion and the oleracein-enriched fraction were tested for their antioxidant potential in the TEAC and DPPH assays. To obtain aglycons of oleraceins, the oleraceins-enriched fraction was treated with the Kiliani reagent (HCl:HCOOH:H_2O) to allow the cleavage of sugar moieties (Mair et al., 2018), resulting in the "hydrolysed fraction" that was also included in the bioactivity assays. In both the TEAC and the DPPH assays, the oleracein-enriched fraction showed better antioxidant activity than the other samples tested, consistent with literature reports on the potent radical scavenging activities of individual oleraceins (Kumar et al., 2022; Jiao et al., 2015). In particular, the fraction showed a TEAC value (2.05 ± 0.05 mg/ml) comparable to that of quercetin 3-*O*-glucoside (TEAC value 1.81 ± 0.009 mM), which was used as a reference compound (Table 2).

3.2.2. Activation of the Nrf2-dependent antioxidant defense

In addition to radical scavenging, the fractions were assessed for their potential to support the enzymatic cellular antioxidant response by activating Nrf2-dependent gene transcription, which is known to maintain the cellular redox balance and to confer protection against oxidative insults in many diseases (Sies et al., 2017). Fig. 4 shows the data obtained for the tested samples regarding the Nrf2 (ARE)-dependent reporter gene (luciferase) expression in stably transfected HepG2 cells. The infusion and oleracein-enriched fraction at 30 μg/mL showed no remarkable activity (activation of 1- and 2-fold of the negative control, respectively), probably due to limited membrane permeation of the highly polar glycosylated components. Accordingly, the hydrolysed fraction at a concentration of 30 μg/ml induced a four-fold activation of the Nrf2 signaling pathway. Looking at the structure of the contained aglycones, the α,β-unsaturated carbonyl group may be responsible for Nrf2 activation due to covalent binding to sensor cysteins of the Nrf2 inhibitor Keap1 (Dinkova-Kostova et al., 2002). Iberin was used as the positive control (3 μM; 5-fold activation). Cell numbers after treatment with the samples tested remained within a range of 85–98% of control cells, excluding major cytotoxic effects.

3.3. Quantitative analysis by LC-ESI/QTrap/MS/MS

To estimate the content of oleraceins, the oleracein-enriched fraction was subjected to semi-preparative RP-HPLC-UV separation, which resulted in the isolation of seven compounds, which were identified by 1D and 2D-NMR and ESI/HRMS^n experiments as the compounds **1**, **3**, **5**, and **9**–**12** by LC-HRMS^n (Table 1), also in agreement with the NMR data reported by Jiao et al. (2015). To determine their amount in the infusion by a specific and sensitive MRM technique, the isolated oleraceins were subjected to tandem mass spectrometric analysis by direct injection in order to define, for each target compound, the transitions to the corresponding product ions to be used in the development of the LC-MS/MS method (Table 3) (Cerulli et al., 2021). In particular, for oleraceins A (**11**), B (**12**), C (**5**), and P (**1**), the transitions generated from the $[M-H]^-$ ion by neutral loss of 162 Da (glucose moiety) (Cerulli et al., 2017) were selected, whereas for oleraceins H (**9**) and I (**10**) neutral losses of 146 Da (coumaroyl moiety) and 176 Da (feruloyl moiety), respectively, were chosen. The 856 → 518 transition was selected for oleracein Q (**3**), whose tandem mass spectrum was characterised by the $[(M-338)-H]^-$ product ion formed by neutral loss of a glucose and a feruloyl moiety linked to each other (Table 3). The results of the quantitative analysis showed that oleracein A was the main compound, followed by oleraceins B and Q, and by oleraceins P, H, I and C, the latter being the least abundant of all (Table 3). Our data were in agreement with the analysis carried out by Fernández-Poyatos et al. (2021) on methanol extracts of raw and steamed aerial parts of *P. oleracea* collected in south-eastern Spain. In this case, the authors made a relative quantitative estimation of each identified compound by calculating the values of the areas (%) of each compound, by using Extracted Ion Chromatograms at the corresponding deprotonated molecule, with respect to the total area. The heatmap obtained scored oleracein A as the main oleracein in both methanolic extracts, followed by oleraceins U, X and Y, then oleracein B, and finally by oleraceins C, J, and N (Fernández-Poyatos et al., 2021). In another work, Petropoulos et al. measured the amount of oleracein A and C in a hydroethanolic extract (ethanol/water 80:20 v/v) obtained from *P. oleracea* leaves collected in Greece at different growth stages, using calibration curves constructed from the UV–VIS signals of a *p*-coumaric acid standard (Petropoulos et al., 2019). In this case, oleraceins A and C were the main oleracein representatives in the leaves, regardless of the stage of harvest (values were in the range of 8.2–103.0 mg and 21.2–143 mg/100 g dry weight, respectively). Finally, in the only other paper reporting an estimation of oleracein content in *P. oleracea*, Jiao et al. used HPLC-UV for quantification and reported an amount of oleracein A and B, ranging from 35.00 to 151.93 mg/kg, and from 40.00 to 150.44 mg/kg, respectively, in the 60% EtOH extract of the aerial parts of *P. oleracea* collected from different regions in China obtained by treatment with ultrasound at room temperature (Jiao et al., 2014). Differences in the content of oleraceins could be attributed to different growing regions and environmental conditions, harvest time and extraction protocols; however, oleracein A always appears as the main oleracein in *P. oleracea*.

Table 2
Antioxidant activity of *Portulaca* infusion and relative fractions.

Tested Samples	DPPH (IC_{50} ± SD[a], μg/ml)	$ABTS^{\bullet+}$ (TEAC ± SD[a], mg/ml)
Infusion	237.75 ± 0.11	0.59 ± 0.11
Oleraceins-enriched fraction	149.32 ± 0.19	2.05 ± 0.25
Hydrolysed fraction	171.21 ± 0.14	0.87 ± 0.11
Ascorbic acid[b]	5.43 ± 0.11 μM	–
Quercetin 3-*O*-glucoside[c]	–	1.81 ± 0.21 μM

[a] SD: Standard deviation of three independent experiments.
[b] Positive control for DPPH assay.
[c] Positive control for TEAC assay.

4. Conclusions

In this study, the infusion from the leaves of *P. oleracea* was defined as the 'green' extract with a high preferential extraction of oleraceins. LC-ESI/HRMS^n spectra analysis of the oleracein-enriched fraction allowed the structural identification of 14 oleraceins, 3 of which not described previously. Moreover, quantitative analysis by LC-MRM-MS defined oleracein A as the most abundant compound among seven isolated and NMR-confirmed oleraceins. At the same time, two fractions obtained from the infusion, i.e. the oleracein-enriched fraction and the hydrolysed fraction, exhibited significant radical scavenging activity *in vitro* and led to activation of the Nrf2 pathway in cells, respectively.

Overall, the results obtained support the use of purslane in the daily diet to benefit from its antioxidant potential, due to its high oleracein content. These results support further detailed study and exploitation of *P. oleracea* or oleraceins for their potential health benefits.

CRediT authorship contribution statement

Ciro Cannavacciuolo: Investigation, Writing – original draft. **Assunta Napolitano:** Investigation, Methodology, Writing – original draft. **Verena M. Dirsch:** Methodology, Investigation. **Elke H. Heiss:** Investigation. **Milena Masullo:** Formal analysis, Writing – review & editing. **Sonia Piacente:** Conceptualization, Funding acquisition, Writing – review & editing.

Table 3
Quantitative determination of oleraceins occurring in the infusion obtained from the leaves of *P. oleracea*.

Compound	MRM transition	Regression Line	R^2	LOD (mg/L)	LOQ (mg/L)	Infusion (mg/100g DW ± SD)[a]
Oleracein A (**11**)	502 → 340	y=(3.91e+2)x-17.1	0.9990	0.06	0.19	445.00 ± 4.33
Oleracein B (**12**)	532 → 370	y=(6.97e+2)x-302	0.9994	0.09	0.30	167.58 ± 5.15
Oleracein C (**5**)	664 → 502	y=(6.45e+4)x+1.29e+4	0.9973	0.11	0.36	13.03 ± 0.46
Oleracein H (**9**)	664 → 518	y=(4.52e+4)x+2.27e+4	0.9986	0.06	0.21	38.58 ± 1.46
Oleracein I (**10**)	694 → 518	y=(5.47e+4)x+4.26 e+4	0.9974	0.08	0.26	24.24 ± 1.14
Oleracein P (**1**)	826 → 664	y=(6.02e+2)x-59.4	0.9990	0.21	0.70	62.08 ± 2.24
Oleracein Q (**3**)	856 → 518	y=(1.85e+2)x-98.8	0.9987	0.06	0.20	113.50 ± 3.89

[a] Values are expressed as mean (mg/100g dried weight) of three experiments ± standard deviation.

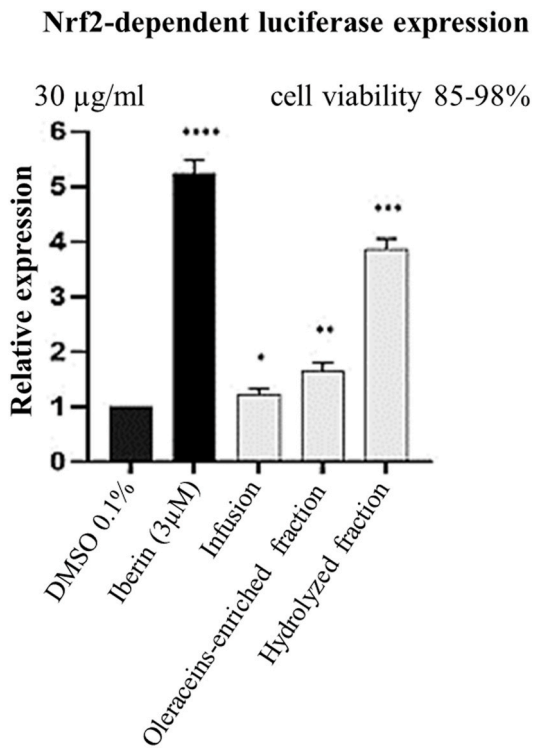

Fig. 4. Activation of the Nrf2 pathway in HepG2-ARE/NRF2-luc cells by purslane leaves infusion and derived fractions. Data are expressed in relative units. Bar graphs represent the transactivation activity expressed as mean ± SD of three independent experiments, n = 3, ****$p < 0.0001$ (One-way ANOVA with Dunnett's post hoc test *vs* vehicle control).

Data availability

Data will be made available on request.

Funding

Project funded under the National Recovery and Resilience Plan (NRRP), Mission 4 Component 2 Investment 1.4—call for tender No. 3138 of December 16, 2021, rectified by Decree n.3175 of December 18, 2021 of the Italian Ministry of University and Research funded by the European Union—NextGenerationEU; Award Number: Project Code CN_00000033, Concession Decree No. 1034 of June 17, 2022 adopted by the Italian Ministry of University and Research, CUP: D43C22001260001, project title "National Biodiversity Future Center—NBFC".

Declaration of competing interest

The authors declare that they have no known competing financial interests or personal relationships that could have appeared to influence the work reported in this paper.

Appendix A. Supplementary data

Supplementary data to this article can be found online at https://doi.org/10.1016/j.crfs.2025.100992.

References

Cannavacciuolo, C., Napolitano, A., Heiss, E.H., Dirsch, V.M., Piacente, S., 2022. *Portulaca oleracea*, a rich source of polar lipids: chemical profile by LC-ESI/LTQOrbitrap/MS/MS and preliminary anti-inflammatory activity. Food Chem. 388, 132968. https://doi.org/10.1016/j.foodchem.2022.132968.

Cerulli, A., Lauro, G., Masullo, M., Cantone, V., Olas, B., Kontek, B., Nazzaro, F., Bifulco, G., Piacente, S., 2017. Cyclic diarylheptanoids from *Corylus avellana* green leafy covers: determination of their absolute configurations and evaluation of their antioxidant and antimicrobial activities. J. Nat. Prod. 80, 1703–1713. https://doi.org/10.1021/acs.jnatprod.6b00703.

Cerulli, A., Napolitano, A., Hosek, J., Masullo, M., Pizza, C., Piacente, S., 2021. Antioxidant and In Vitro Preliminary Anti-Inflammatory Activity of *Castanea sativa* (Italian Cultivar "Marrone di Roccadaspide" PGI) Burs, Leaves, and Chestnuts Extracts and Their Metabolite Profiles by LC-ESI/LTQOrbitrap/MS/MS. Antioxidants 10, 278. https://doi.org/10.3390/antiox10020278.

Cerulli, A., Napolitano, A., Olas, B., Masullo, M., Piacente, S., 2023. *Corylus avellana* "Nocciola Piemonte": metabolomics focused on polar lipids and phenolic compounds in fresh and roasted hazelnuts. Front. Plant Sci. 14, 1252196. https://doi.org/10.3389/fpls.2023.1252196.

Cuadrado, A., Rojo, A.I., Wells, G., Hayes, J.D., Cousin, S.P., Rumsey, W.L., Attucks, O.C., Franklin, S., Levonen, A.L., Kensler, T.W., Dinkova-Kostova, A.T., 2019. Therapeutic targeting of the NRF2 and KEAP1 partnership in chronic diseases. Nat. Rev. Drug Discov. 18, 295–317. https://doi.org/10.1038/s41573-018-0008-x.

D'Urso, G., Napolitano, A., Cannavacciuolo, C., Masullo, M., Piacente, S., 2020. Okra fruit: LC-ESI/LTQOrbitrap/MS/MS based deep insight on polar lipids and specialized metabolites with evaluation of anti-oxidant and anti-hyperglycemic activity. Food Funct. 11, 7856–7865. https://doi.org/10.1039/d0fo00867b.

Dinkova-Kostova, A.T., Holtzclaw, W.D., Cole, R.N., Itoh, K., Wakabayashi, N., Katoh, Y., Yamamoto, M., Talalay, P., 2002. Direct evidence that sulfhydryl groups of Keap1 are the sensors regulating induction of phase 2 enzymes that protect against carcinogens and oxidants. Proc. Natl. Acad. Sci. U.S.A. 99, 11908–11913. https://doi.org/10.1073/pnas.172398899.

Farag, M.A., Shakour, Z.T.A., 2019. Metabolomics driven analysis of 11 *Portulaca* leaf taxa as analysed UPLC-ESI-MS/MS and chemometrics. Phytochemistry 161, 117–129. https://doi.org/10.1016/j.phytochem.2019.02.009.

Fernández-Poyatos, M.D., Llorent-Martínez, E.J., Ruiz-Medina, A., 2021. Phytochemical composition and antioxidant activity of *Portulaca oleracea*: influence of the steaming cooking process. Foods 10, 94. https://doi.org/10.3390/foods10010094.

Iranshahy, M., Javadi, B., Iranshahi, M., Jahanbakhsh, S.P., Mahyari, S., Hassani, F.V., Karimi, G., 2017. A review of traditional uses, phytochemistry and pharmacology of *Portulaca oleracea* L. J. Ethnopharmacol. 205, 158–172. https://doi.org/10.1016/j.jep.2017.05.004.

Jiao, Z., Wang, H., Wang, P., Sun, H., Yue, S., Xiang, L., 2014. Detection and quantification of cyclo-dopa amides in *Portulaca oleracea* L. by HPLC-DAD and HPLC-ESI-MS/MS. J. Chin. Pharmaceut. Sci. 23, 533–542. https://doi.org/10.5246/jcps.2014.08.069.

Jiao, Z.Z., Yue, S., Sun, H.X., Jin, T.Y., Wang, H.N., Zhu, R.X., Xiang, L., 2015. Indoline amide glucosides from *Portulaca oleracea*: isolation, structure, and DPPH radical scavenging activity. J. Nat. Prod. 78, 2588–2597. https://doi.org/10.1021/acs.jnatprod.5b00524.

Kumar, A., Sreedharan, S., Kashyap, A.K., Singh, P., Ramchiary, N., 2022. A review on bioactive phytochemicals and ethnopharmacological potential of purslane (*Portulaca oleracea* L.). Heliyon 8, e08669. https://doi.org/10.1016/j.heliyon.2021.e08669.

Ma, H., Chen, X., Zhang, X., Wang, Q., Mei, Z., Li, L., Liu, Y., 2024. Transcriptomic analysis reveals antibacterial mechanism of probiotic fermented *Portulaca oleracea* L. against *Cronobacter sakazakii* and application in reconstituted infant formula. Food Biosci. 58, 103721. https://doi.org/10.1016/j.fbio.2024.103721.

Mair, C.E., Grienke, U., Wilhelm, A., Urban, E., Zehl, M., Schmidtke, M., Rollinger, J.M., 2018. Anti-influenza triterpene saponins from the bark of burkea africana. J. Nat. Prod. 81, 515–523. https://doi.org/10.1021/acs.jnatprod.7b00774.

Melilli, M.G., Pagliaro, A., Scandurra, S., Gentile, C., Di Stefano, V., 2020. Omega-3 rich foods: durum wheat spaghetti fortified with *Portulaca oleracea*. Food Biosci. 37, 100730. https://doi.org/10.1016/j.fbio.2020.100730.

Moneim, A.E.A., 2013. The neuroprotective effects of purslane (*Portulaca oleracea*) on rotenone-induced biochemical changes and apoptosis in brain of rat. Cns Neurol. Disord. Drug Targets 12, 830–841. https://doi.org/10.2174/18715273113129990081.

Moneim, A.E.A., Dkhil, M.A., Al-Quraishy, S., 2013. The potential role of *Portulaca oleracea* as a neuroprotective agent in rotenone-induced neurotoxicity and apoptosis in the brain of rats. Pestic. Biochem. Physiol. 105, 203–212. https://doi.org/10.1016/j.pestbp.2013.02.004.

Nemzer, B., Al-Taher, F., Abshiru, N., 2020. Phytochemical composition and nutritional value of different plant parts in two cultivated and wild purslane (*Portulaca oleracea* L.) genotypes. Food Chem. 320, 126621. https://doi.org/10.1016/j.foodchem.2020.126621.

Petropoulos, S.A., Fernandes, Â., Dias, M.I., Vasilakoglou, I.B., Petrotos, K., Barros, L., Ferreira, I.C.F.R., 2019. Nutritional value, chemical composition and cytotoxic properties of common purslane (*Portulaca oleracea* L.) in relation to harvesting stage and plant part. Antioxidants 8, 293. https://doi.org/10.3390/antiox8080293.

Rahimi, V.B., Ajam, F., Rakhshandeh, H., Askari, V.R., 2019. A pharmacological review on Portulaca oleracea L.: focusing on anti-inflammatory, anti-oxidant, immunomodulatory and antitumor activities. J. Pharmacopuncture 22, 7–15. https://doi.org/10.3831/Kpi.2019.22.001.

Sies, H., Berndt, C., Jones, D.P., 2017. Oxidative stress. Annu. Rev. Biochem. 86, 715–748. https://doi.org/10.1146/annurev-biochem-061516-045037.

Sun, H., He, X., Liu, C., Li, L., Zhou, R., Jin, T., Yue, S., Feng, D., Gong, J., Sun, J., Ji, J., Xiang, L., 2017. Effect of oleracein E, a neuroprotective tetrahydroisoquinoline, on rotenone-induced Parkinson's disease cell and animal models. ACS Chem. Neurosci. 8, 155–164. https://doi.org/10.1021/acschemneuro.6b00291.

Tanaka, Y., Sasaki, N., Ohmiya, A., 2008. Biosynthesis of plant pigments: anthocyanins, betalains and carotenoids. Plant J. 54, 733–749. https://doi.org/10.1111/j.1365-313X.2008.03447.x.

Truong, H.K.T., Huynh, M.A., Vuu, M.D., Dang, T.P.T., 2019. Evaluating the potential of *Portulaca oleracea* L. For Parkinson's disease treatment using a Drosophila model with dUCH-knockdown. Parkinson's Dis. 2019, 1818259. https://doi.org/10.1155/2019/1818259.

Voynikov, Y., Nedialkov, P., Gevrenova, R., Zheleva-Dimitrova, D., Balabanova, V., Dimitrov, I., 2021. UHPLC-Orbitrap-MS tentative identification of 51 oleraceins (Cyclo-Dopa amides) in *Portulaca oleracea* L. Cluster analysis and MS filtering by mass difference. Plants 10, 1921. https://doi.org/10.3390/plants10091921.

Wang, C.Q., Yang, G.Q., 2010. Betacyanins from *Portulaca oleracea* L. ameliorate cognition deficits and attenuate oxidative damage induced by D-galactose in the brains of senescent mice. Phytomedicine 17, 527–532. https://doi.org/10.1016/j.phymed.2009.09.006.

Wang, W.Y., Gu, L.M., Dong, L.W., Wang, X.L., Ling, C.Q., Li, M., 2007. Protective effect of *Portulaca oleracea* extracts on hypoxic nerve tissue and its mechanism. Asia Pac. J. Clin. Nutr. 16, 227–233.

Xiang, L., Xing, D.M., Wang, W., Wang, R.F., Ding, Y., Du, L.J., 2005. Alkaloids from *Portulaca oleracea* L. Phytochemistry 66, 2595–2601. https://doi.org/10.1016/j.phymed.2009.09.006.

Yang, Y., Zhou, X., Jia, G., Zhao, H., Li, Y., Cao, J., Guan, Z., Zhao, R., 2024. *Portulaca oleracea* L. polysaccharide ameliorates ulcerative colitis by regulating the immune system and gut microbiota. Food Biosci. 61, 104926. https://doi.org/10.1016/j.fbio.2024.104926.

Zhang, H.X., Yu, N.C., Huang, G.F., Shao, J.B., Wu, Y.X., Huang, H.J., Liu, Q., Ma, W., Yi, Y.D., Huang, H., 2007. Neuroprotective effects of purslane herb aquenous extracts against D-galactose induced neurotoxicity. Chem. Biol. Interact. 170, 145–152. https://doi.org/10.1016/j.cbi.2007.07.009.

Zhang, H., Chen, G., Yang, J., Yang, C., Guo, M., 2022. Screening and characterisation of potential antioxidant, hypoglycemic and hypolipidemic components revealed in *Portulaca oleracea* via multi-target affinity ultrafiltration LC-MS and molecular docking. Phytochem. Anal. 33, 272–285. https://doi.org/10.1002/pca.3086.